

Earth and Space Science



RESEARCH ARTICLE

10.1029/2023EA002927

Key Points:

- We found a b -value precursor that coincides with foreshocks for 2 days before the 2018 M_L 6.3 Hualien earthquake in the source area
- The b -value precursor correlates with foreshock distribution in the source area and is likely uncorrelated to the high coseismic slip
- There is no significant change in the b -value before $M \geq 6.0$ earthquakes in Taiwan in a majority of the cases that we analyzed

Supporting Information:

Supporting Information may be found in the online version of this article.

Correspondence to:

S. K. Chen,
sean80254@gmail.com

Citation:

Chen, S. K., Chen, P.-Y., Wu, Y.-M., Chen, C.-C., & Chan, C.-H. (2023). Temporal variations of earthquake magnitude-frequency relation in the source area of $M \geq 6.0$ earthquakes: A systematic survey in Taiwan. *Earth and Space Science*, 10, e2023EA002927. <https://doi.org/10.1029/2023EA002927>

Received 8 MAR 2023
Accepted 13 NOV 2023

Author Contributions:

Conceptualization: Sean Kuanhsiang Chen
Formal analysis: Sean Kuanhsiang Chen, Po-Yuan Chen, Yih-Min Wu
Investigation: Sean Kuanhsiang Chen, Po-Yuan Chen, Yih-Min Wu
Methodology: Sean Kuanhsiang Chen, Po-Yuan Chen
Validation: Chien-Chih Chen, Chung-Han Chan
Writing – original draft: Sean Kuanhsiang Chen

Temporal Variations of Earthquake Magnitude-Frequency Relation in the Source Area of $M \geq 6.0$ Earthquakes: A Systematic Survey in Taiwan

Sean Kuanhsiang Chen¹ , Po-Yuan Chen¹, Yih-Min Wu^{1,2,3}, Chien-Chih Chen⁴ , and Chung-Han Chan^{4,5}

¹Department of Geosciences, National Taiwan University, Taipei, Taiwan, ²Institute of Earth Sciences, Academia Sinica, Taipei, Taiwan, ³Research Center for Future Earth, National Taiwan University, Taipei, Taiwan, ⁴Department of Earth Sciences, National Central University, Taoyuan, Taiwan, ⁵Earthquake-Disaster & Risk Evaluation and Management Center, National Central University, Taoyuan, Taiwan

Abstract Recent studies in the earthquake magnitude-frequency relation (b -value) found that the b -value can decrease with time before large earthquakes in the source area. Such a decrease even coincided with a burst of foreshocks immediately before the earthquakes implying a preslip migrating toward the nucleation zone. We systematically survey the b -value variations in space and time in the source area of 17 earthquakes with magnitudes greater than M_L 6.0 in Taiwan. We relocated the earthquakes released by the Central Weather Administration of Taiwan since 2012 as timing can provide a sufficiently low completeness magnitude (M_C) of 1.5. We carefully determine the spatiotemporal search criteria on seismicity in the source area of all targeted earthquakes. We surveyed the temporal b -value systematically using moving time windows with a given number of earthquake events with the magnitudes greater than M_C . We found the b -value decreased clearly for 2 days before the 2018 M_L 6.3 Hualien earthquake, coinciding with a burst of M_L 5.8 earthquake and its aftershocks nearby as foreshocks. The foreshocks migrated updip toward the hypocenter of the 2018 M_L 6.3 Hualien earthquake and revealed a second decrease in the b -value 10 hours before it occurred. The b -value precursor primarily comes from a rapid reduction of small earthquakes in the foreshocks and agrees with recent key findings of preslip. However, there is no strong correlation between the b -value precursor and coseismic slip. Apart from this, the b -values did not change significantly in most cases of earthquakes in Taiwan before and after they occurred.

Plain Language Summary Direct evidence for the precursor of a large earthquake is rare and difficult to be quantified accurately. Earthquake magnitude-frequency relation (b -value) is a classic observation implying stress accumulation on a seismogenic fault. Scientists found that the b -value can decrease within a few days before an impending large earthquake in the source area. Taiwan is one of the regions undergoing frequent $M \geq 6.0$ earthquakes and can map the b -value in high resolution based on the relocated earthquakes. This study systematically surveyed the b -value in the source area of seventeen $M_L \geq 6.0$ earthquakes in Taiwan, probing into b -value precursor in the 8-year time series. We found that the b -value had a robust decrease 2 days before the 2018 M_L 6.3 Hualien earthquake, coinciding with the initiation of foreshocks nearby and a downdip of the hypocenter of the 2018 M_L 6.3 Hualien earthquake. The foreshocks showed clear evidence of precursor as they migrated updip toward the hypocenter with a second decrease in the b -value 10 hours before the earthquake occurred. We found no evidence of a b -value precursor in most of the targeted earthquakes that agrees with the knowledge of precursor as happening episodically and unexpectedly.

1. Introduction

Earthquake magnitude-frequency relation in global seismogenic crust typically follows the Gutenberg-Richter Law: $\log_{10} N = a - bM$ (Gutenberg & Richter, 1944), where the b -value represents the frequency of small to large earthquakes empirically shown as 1.0 (e.g., Petruccioli et al., 2019; Schorlemmer et al., 2005). The b -value varies primarily with differential stress in the crust and shows an inverse relation to the differential stress in worldwide observations (e.g., Dal Zillo et al., 2018; Scholz, 2015; Spada et al., 2013). Laboratory acoustic emissions have shown that the b -value decreases with stress accumulation on rock samples before the fracture develops (e.g., Amitrano, 2003; Goebel et al., 2013; Scholz, 1968). However, such a temporal variation of the b -value was not

© 2023 The Authors.

This is an open access article under the terms of the [Creative Commons Attribution-NonCommercial License](https://creativecommons.org/licenses/by/4.0/), which permits use, distribution and reproduction in any medium, provided the original work is properly cited and is not used for commercial purposes.

Writing – review & editing: Yih-Min Wu, Chien-Chih Chen, Chung-Han Chan

much before the earthquake fracture. Some studies found that the b -value can decrease before large earthquakes from several months to years ago in the source area (e.g., Chen & Zhu, 2020; Nanjo, 2020; Schurr et al., 2014; Tormann et al., 2015). In the 2011, M_w 9.0 Tohoku-Oki and 2014 M_w 8.1 Iquique earthquakes, the decreasing b -value was observed primarily at an area of high coseismic slip (e.g., Schurr et al., 2014; Tormann et al., 2015) implying a process of stress accumulation on the fault asperities (Hashimoto et al., 2009; Nanjo & Yoshida, 2018; Wiemer & Wyss, 1997). Temporal evolution of the b -value and how significant that can be as a precursor of a large earthquake remains unclear. Aftershocks can relieve some of the accumulated stress on an entire seismogenic fault around the coseismic slip (e.g., Bilek & Lay, 2018; Toda & Stein, 2022). Gulia et al. (2018) stacked 58 aftershock sequences following worldwide M_w 6.0 to 8.0 earthquakes, showing that the b -value can increase immediately after the earthquakes in the source area by 20% and then decrease slowly with time return to the pre-earthquake background level. This study suggests that how the b -value decreases with time may rely on the earthquake magnitude, faulting style, and spatial search criteria of the b -value. Gulia and Wiemer (2019) found that the b -value can decrease by over 10% less than the pre-earthquake background level during aftershocks and soon happened a great earthquake, as observed in the cases of 2011 M_w 9.0 Tohoku-Oki, 2016 M_w 7.3 Kumamoto, and 2019 M_w 7.1 Ridgecrest earthquakes. Such a b -value decrease outside the preexisting source areas could be a mechanism of preslip migrating toward the nearby fault asperities (Gulia & Wiemer, 2019; Nanjo, 2020; Nanjo et al., 2019). However, knowledge of the b -value precursor and its linkage to preslip remains limited.

Taiwan is a young orogen converging with a rate of approximately 80 mm/yr between the Philippine Sea Plate and the Eurasian Plate (e.g., Chen et al., 2017; Hsu et al., 2009; Yu et al., 1997). The rapid convergence rate causes thousands of earthquakes annually in the orogenic crust and the two subduction zones (Figure 1). The 1999 M_w 7.6 Chi-Chi earthquake took away over 2,400 people in Taiwan. A recent 2016 M_w 6.4 Meinong earthquake also caused 117 deaths. A systematic temporal b -value survey in the source areas of large earthquakes is crucial to seismic hazard mitigation in Taiwan. The b -value was estimated to be approximately 0.6–1.5 in the orogenic crust and offshore regions (e.g., Chan et al., 2012; Wang, 1988; Wang et al., 2015; Wu Y. H. et al., 2013; Wu Y. M. et al., 2018). Before the 1999 M_w 7.6 Chi-Chi earthquake, Wu and Chiao (2006) found that the b -value was likely to decrease with time in the source area since a few months ago, that happened similarly before another 2003 M_w 6.8 Chengkung earthquake (Wu, Chen, et al., 2008). Chan et al. (2012) analyzed the b -value before twenty-three M_L 6.0 to 7.3 earthquakes in Taiwan, showing the b -value decrease seemed to frequently precede 12 of the earthquakes in the last year before their occurrence. However, the temporal resolution of the b -value was a monthly to yearly scale, which made it difficult to validate the b -value precursor in the source area. The Central Weather Administration (CWA) of Taiwan established a whole-island seismic network in Taiwan in 1991, so-called the CWASN afterward. The completeness of earthquake magnitude (M_C) was 2.2 in the orogenic crust and 2.2 to 3.4 in the offshore regions from the CWASN catalog (Chan et al., 2012). After a systematical update of the CWASN to a 100 Hz sampling rate and 24-bit computing in 2012, we have gained an improvement of M_C by 1.5 inland and approximately 1.5–2.5 offshore (Figure 2). This improvement advantages a higher temporal resolution of the b -value in the source area. Previous studies in Taiwan have estimated the temporal b -value by time-fixed windows in the source area of $M_L \geq 6.0$ earthquakes (Chan et al., 2012; Wu & Chiao, 2006; Wu, Chen, et al., 2008). We use moving time windows and constrain the window length by a threshold of earthquake event number for the b -value estimates. It ensures the time window is flexible and sensitive to the seismicity rate change before a large earthquake if any b -value precursor or foreshocks happen (e.g., Chen & Zhu, 2020; Gulia & Wiemer, 2019; Nanjo et al., 2012; Tormann et al., 2015).

2. Data and Methods

2.1. Earthquake Data and Spatiotemporal Search Criteria for the b -Value

We relocated 319,245 earthquakes from the CWASN earthquake catalog from 2012 to 2019 in Taiwan by the approach of Wu, Chang, et al. (2008). We reduced the uncertainties of the earthquake hypocenters significantly by less than 3 and 5 km in horizontal and vertical space, respectively. In the Taiwan orogen, the thickened crust can extend to approximately a 30 km depth in the northern and southern segments and down to over 45 km in the central (e.g., Huang et al., 2014; Kuo-Chen et al., 2012; Wu et al., 2007). We focus on seventeen $M_L \geq 6.0$ earthquakes in the crust and survey the temporal b -value in the source area over the 8-year seismicity (Figure 1). We select 294,840 relocated earthquakes above the depth of 40 km for estimating the b -value, considering the source depth from the targeted earthquakes into account. We survey the b -value in Taiwan in three steps: (a) Estimating the b -value and M_C distributions in homogeneous spacing grids. (b) Determining spatial search criteria of the b -value for the seventeen $M_L \geq 6.0$ earthquakes in the source area. (c) Calculating temporal b -value by moving

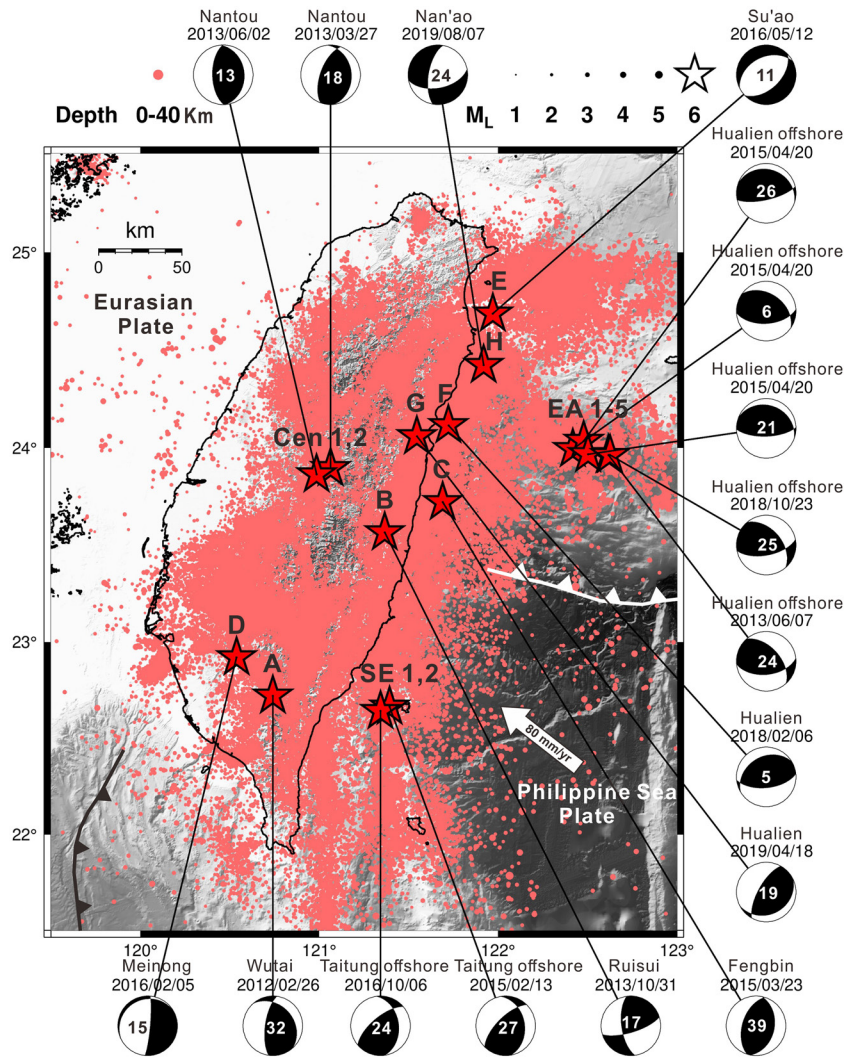


Figure 1. Tectonics and relocated earthquakes in Taiwan from 2012 to 2019 at depths shallower than 40 km. The red stars represent epicenters of 17 targeted $M_L \geq 6.0$ earthquakes. The number at the center of each focal mechanism is the source depth. We use the label at the head of each epicenter in substitution for the earthquakes in Figure 3.

time windows in the source area. We estimate the b -value and M_C using a radius from the grid center, which covers all relocated earthquakes from the surface to 40 km depth as in a cylinder. To show an improvement in earthquake detectability in this study, we estimated the M_C under a homogeneous 0.2° -spacing grid, the same as previous studies in Taiwan (Chan et al., 2012; Wu & Chiao, 2006; Wu, Chen, et al., 2008) and further went into a 0.1° -spacing grid. We determine the b -value using the maximum likelihood method (Aki, 1965): $b = \frac{\log_{10} c}{M - M_{\min}}$, where M_{\min} is the M_C in the relocated earthquakes. \bar{M} is the average magnitude of all relocated earthquakes from the magnitudes over M_C . We determine M_C using the maximum curvature method (Wiemer & Wyss, 2000) that requires at least 100 events over the M_C in each grid cell. Several studies increased the cut-off of M_C by 0.2 and examined the reproducibility of the b -value to ensure that M_C determination is robust enough (e.g., Gulia et al., 2018; Nanjo et al., 2012; Petrucci et al., 2019; van der Elst, 2021; Woessner & Wiemer, 2005). However, previous studies in Taiwan did not consider such an increase in the cut-off of M_C in the b -value estimates (e.g., Chan et al., 2012; Wu & Chiao, 2006; Wu, Chen, et al., 2008). To this end, we determine the b -value by the original M_C to be comparable to the previous studies and by an extra cut-off increase of 0.2.

This study uses a radius from the epicenter to calculate the b -value in the source area of the targeted earthquakes because the fault geometry of most targeted earthquakes remains unclear. To search for a radius appropriate for the source area, we examine the b -value under 15–50 km radiuses in time-fixed windows every half a year

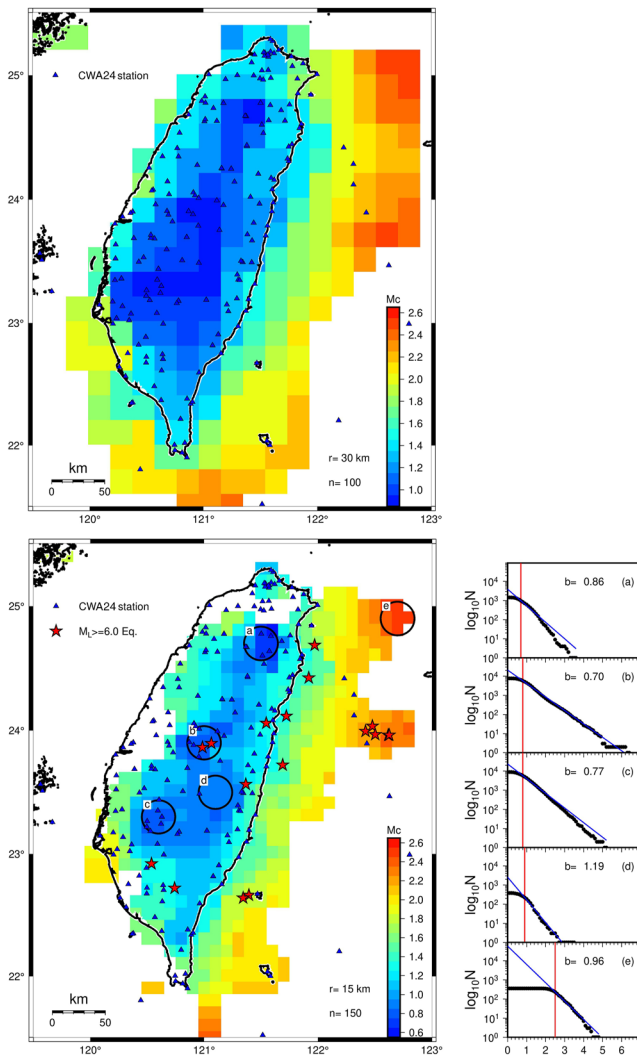


Figure 2. The magnitude of completeness (M_C) in the space under the Central Weather Administration 24-bits (CWA24) seismic network. (a) The M_C distribution before 2012 derived from the spatial search criteria of seismicity previously (see Introduction for details). (b) New M_C distribution determined in this study. We show several examples of the robust b -value and M_C estimates in the magnitude-frequency relations as the blue and red lines, respectively. The circles in the M_C map represent the coverage of seismicity in the space as the black dots in the cumulative number of earthquakes.

preliminarily. Each time window requires at least 50 events in the cylinder with their magnitudes over an extra cut-off increase of 0.2 in M_C to stabilize the b -value estimates (e.g., Nanjo et al., 2012; Tormann et al., 2015; Woessner & Wiemer, 2005). To assess the temporal resolution of the b -value in the source area, we examine how many events are over the magnitude threshold in each time window if the radius from the epicenter changes. We observe that the b -value can be resolved coherently by a radius of 20–25 km for the $M_L \geq 6.0$ earthquakes in the inland areas (Figure 3). The radius of 25 km constrains the b -value well in every time window, which is reproducible by the radius of 20 km for only a few missing b -values in the time windows (Figure 3). In the offshore areas, the b -value requires a much longer radius from the epicenter to satisfy the threshold of event number in the cylinder. It is not surprising the longer the radius, the higher the number of events over the magnitude threshold for the time window (Chen & Zhu, 2020; Nanjo, 2020; Woessner & Wiemer, 2005). We use the radius of 20 km to survey the temporal b -value systematically if a search radius small enough to the nucleation zone can illuminate the b -value change (e.g., Chen & Zhu, 2020; Nanjo, 2020; Tormann et al., 2015). Note this radius only ensures a high-resolution b -value mapping in the source area of inland earthquakes.

Besides, aftershocks typically occur in a region broader than the source area of a large earthquake (e.g., Bilek & Lay, 2018; Toda & Stein, 2022). A search radius much longer is needed to cover the aftershocks following the seventeen $M_L \geq 6.0$ earthquakes. We calculate the b -value under a radius at least twice to fourth the 20 km following the earthquakes in the half-year time windows. We observe that a radius of 50 km from the epicenter can cover the aftershocks coherently from the targeted earthquakes (Figure 4). Some aftershocks away from the source area will be lost if the search radius is less than 40 km. Also, there will be no clear seismicity at the edge of the cylinders if it is over 60 km. The number of aftershocks decreases significantly with the radius from the epicenter in most targeted earthquakes. The rate of aftershocks commonly increases rapidly after the targeted earthquakes and decays to the background seismicity in a week (Figure 4). Some aftershock sequences are much longer than a week, like after the 2013 M_L 6.4 Ruisui, 2016 M_L 6.6 Meinong, and 2018 M_L 6.3 Hualien earthquakes (Figure S1 in Supporting Information S1).

2.2. Moving Time-Windows Setting for a Temporal b -Value Survey

Next, we survey the temporal b -value in the source area of the targeted earthquakes by two radiuses of 20 and 50 km from the epicenter using moving time windows. To reduce the heterogeneity of temporal variations in M_C in the source area, we searched for a coherent M_C over the whole periods in the earthquake catalog named precutting level (Gulia et al., 2018; Nanjo et al., 2012; Tormann et al., 2015). Then, we establish each time window by at least 50 events with their magnitudes over an extra cut-off increase of 0.2 in the precutting level to obtain a reliable b -value (e.g., Gulia et al., 2018; Gulia & Wiemer, 2019; Nanjo, 2020). We quantify the uncertainties of the temporal b -value using the method of Shi and Bolt (1982). Previous studies overlapped the time windows for 50%, 75%, or nearly whole (95%) to ensure the b -value changes continuously with time, not dramatically (Chen & Zhu, 2020; García-Hernández et al., 2021; Gulia et al., 2018; Tormann et al., 2015). Note in Section 2.1, the time window is non-overlapped for the b -value estimates. Here, we examine the overlapping degree between each time window in 0%, 50%, 75%, and 95% to see how the b -value varies with time linked to the targeted earthquakes. We set the first time window at the earthquake occurrence time and left the following windows away from the first one by the given overlapping degrees. This setting advantages a detailed temporal mapping in the b -value before and after a large earthquake. We determine an overlapping degree appropriate for the local seismicity rate in Taiwan

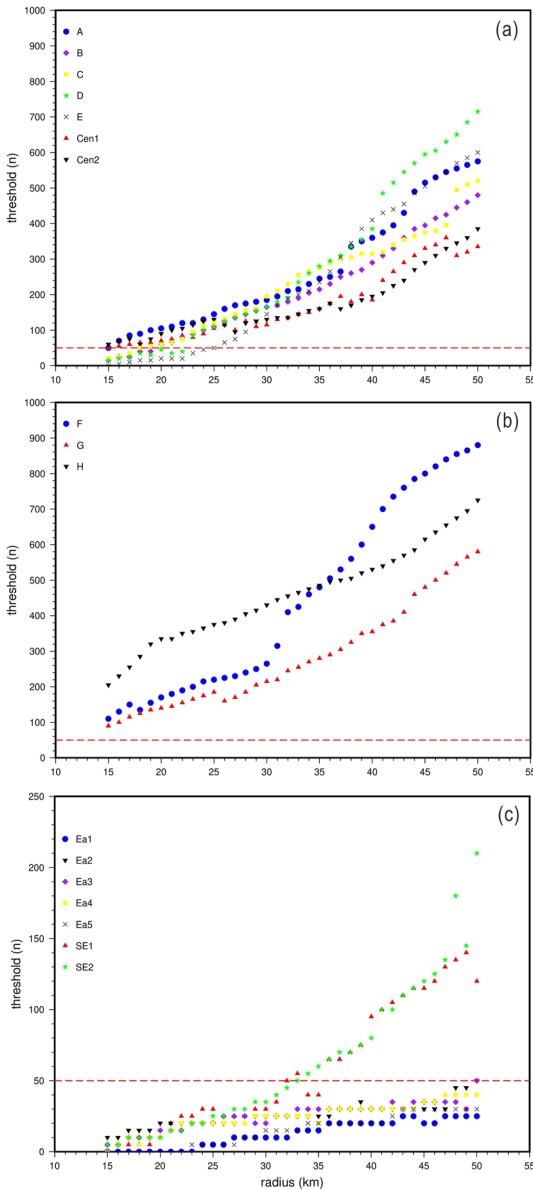


Figure 3. Relationship between the search radius from the epicenter of 17 targeted $M_L \geq 6.0$ earthquakes (Figure 1) and the earthquake events with magnitudes greater than M_C . The red dotted lines represent a threshold of at least 50 earthquake events over the M_C in the source area.

by a similarity between the b -value time series (e.g., Chen & Zhu, 2020; García-Hernández et al., 2021; Gulia et al., 2018). The similarity means how a b -value time series determined from one overlapping degree correlates to its 95%-overlapping time series. The correlation will be 100% ($r = 1$) if the b -value time series are both under an overlapping degree of 95%, and we require $r = 0.9$ to avoid artifacts and misinterpretation. To carefully constrain the moving time windows, we examine how the temporal b -value varies with the event number in each time window under an overlapping degree. We request at least 50 to 230 events with their magnitudes over an extra cut-off increase of 0.2 in the precutting level.

3. Results

3.1. New b -Value Maps in Taiwan

Figure 5 shows four b -value maps in a homogeneous 0.1° -spacing grid determined by various search radiuses. It is clear the b -value distribution in space increases with the search radius from 15 to 30 km (Figures 5a–5c) due to a long search radius capturing more seismicity. However, such an increase in search radius also reduces the heterogeneity of the b -value and may lead to the b -values being inaccurate (e.g., García-Hernández et al., 2021; Nanjo, 2020; Nanjo & Yoshida, 2018). We found that the heterogeneity of the b -value is visible under a search radius of 15 and 20 km (Figures 5b and 5c). The heterogeneity seems to stay still when we raise the event number with their magnitudes over a magnitude threshold from 100 to 150 under the radius of 15 km (Figures 5c and 5d). This spatial search criterion also reduces some b -values that may be uncertain in Figure 5c in northern Taiwan and offshore regions. Thus, we use the b -value map in Figure 5d for interpretations in the following. It shows that the b -values are commonly higher at 1.1 to 1.4 in northern Taiwan and the offshore area, regionally lower at 0.7 to 0.8 in central to southern Taiwan. The b -values are lowest at 0.5 in the eastern offshore region in the source area of five $M_L \geq 6.0$ earthquakes (Figure 5d). We have validated these b -values from the stable slopes in their magnitude-frequency relations (Figure 2). The new b -value map shows a distribution of 0.5–1.4 in a resolution higher than previous studies and slightly lower than the estimates of 0.6–1.5 (e.g., Chan et al., 2012; Wang, 1988; Wang et al., 2015; Wu, Chen, et al., 2008). A decrease of M_C from the CWASN in this study could be a reason for the systematical difference. There is another possibility that the previous estimates involved many aftershocks from the 1999 M_w 7.6 Chi-Chi earthquake in Taiwan. The effect of Chi-Chi aftershocks may last over a decade in the orogenic crust (Lee et al., 2013). Our choice of earthquake data since 2012, at least 13 years after Chi-Chi, can significantly reduce such an effect. Note the targeted earthquakes in this study almost occurred in a region where the b -value is lower than the surroundings (red stars in Figure 5d). It is consistent with previous findings that a large earthquake tends to happen in a place of low b -value regionally (e.g., Chan et al., 2012; Nanjo & Yoshida, 2018; Schurr et al., 2014; Tormann et al., 2015).

3.2. Resolution and Temporal Variations of b -Value in the Source Area of $M_L \geq 6.0$ Earthquakes

Here we show the b -value time series in the source area of the targeted earthquakes under a half-year time-fixed window as evidence related to Figure 3. In Figure S2 of Supporting Information S1, the b -value can be resolved in every time window under a search radius of 25 km for all the inland earthquakes. A radius of 20 km can perform this result similarly but not under a much smaller radius. The b -value cannot be resolved in many time windows if the radius equals or is smaller than 15 km for the inland earthquakes (Figure S2 in Supporting Information S1). Thus, we chose a radius of 20 km for a systematical b -value survey in the source area. The temporal b -value

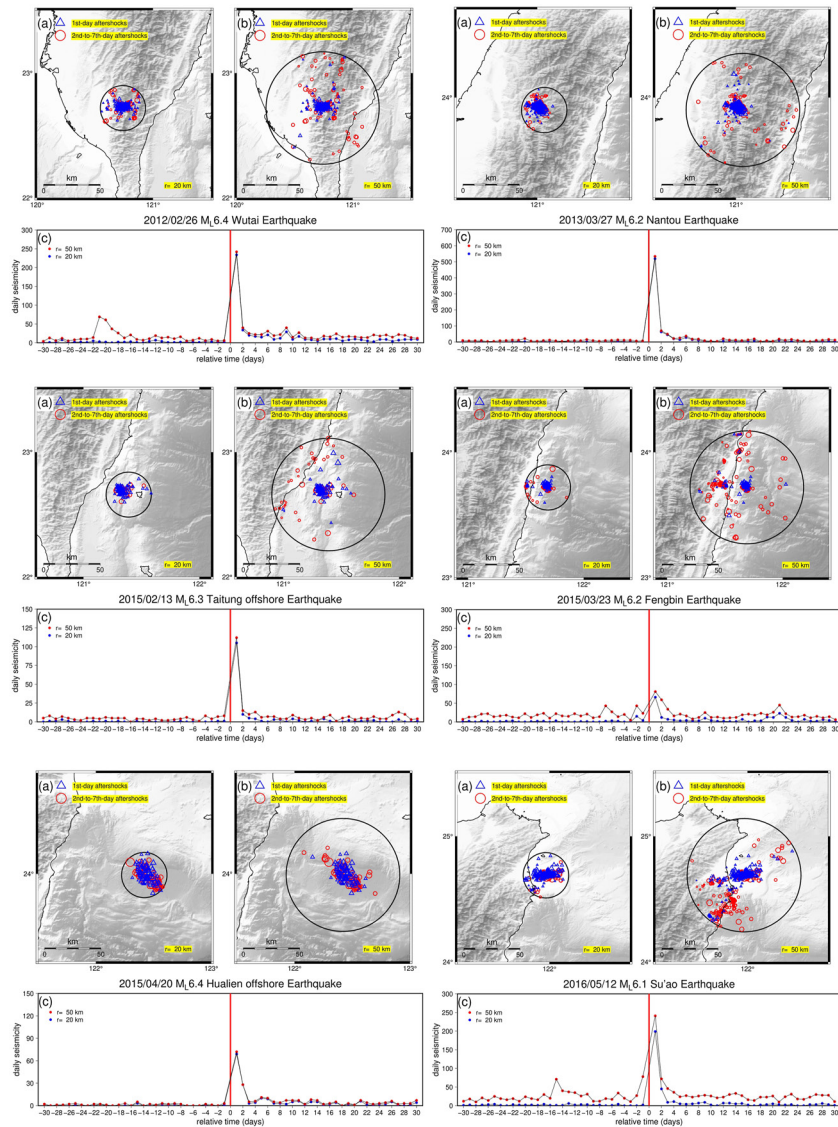


Figure 4. Aftershock distribution in the space and time from six of the targeted $M_L \geq 6.0$ earthquakes. The spatial distribution is shown in search radiuses of 20 and 50 km from the epicenter in subfigure (a) and (b), respectively. The temporal evolution of aftershocks is shown in subfigure (c) under the two search radiuses with background seismicity. The red lines are the earthquake occurrence times. See Supporting Information S1 for the other cases.

likely varies with the search radius from the epicenter in several source areas, like the 2012 M_L 6.4 Wutai, 2013 Nantou M_L 6.5, and 2019 M_L 6.3 Nan'ao earthquakes (Figure S2 in Supporting Information S1). The half-year time series likely reveal a decrease of the temporal b -value before the 2018 M_L 6.3 Hualien earthquake from a pre-earthquake background level of 0.85 to 0.65 (Figure S2 in Supporting Information S1). Such a decrease in the b -value is visible coherently in various search radiuses from the epicenter. However, the temporal resolution is not precise enough to indicate any significant meanings of the b -value change. We note the temporal b -value is poorly constrained for offshore earthquakes and does not show under this search radius.

Figure 6 shows the b -value time series from various overlapping degrees between each time window under a search radius of 20 km from the epicenters inland. The temporal b -value can vary coherently over the 8-year time series under different overlapping degrees. A higher overlapping degree shows a more detailed variation. We found that the similarity of the b -value time series commonly reaches 0.9 in the 75% overlapping with a b -value uncertainty of ± 0.06 (Figure 6). It can be down to ± 0.05 but requires considerable computing costs if the overlapping degree reaches 95%. An overlapping degree of 50% can relieve much of the computing costs, but the

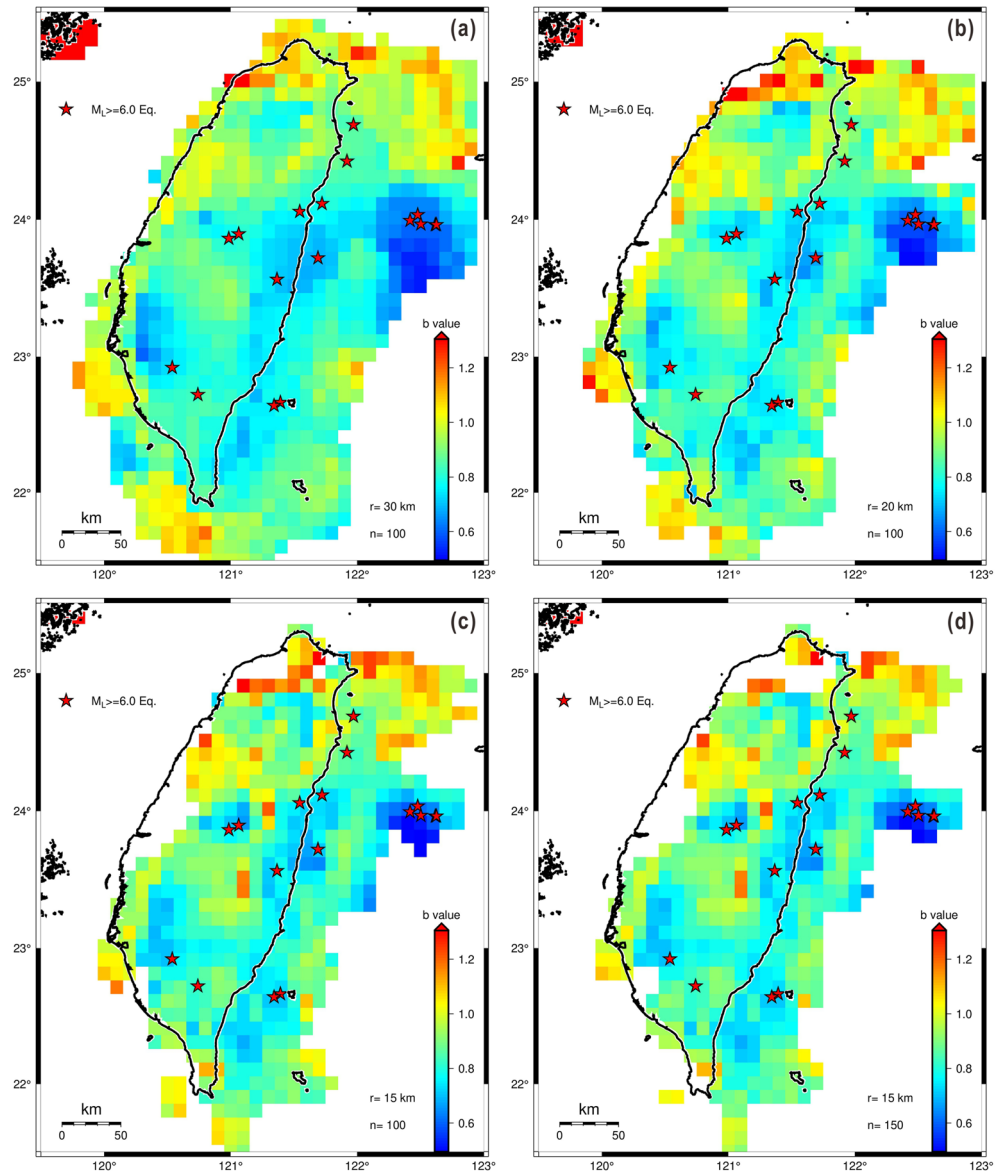


Figure 5. New b -value maps in Taiwan derived from relocated earthquakes from 2012 to 2019. (a)–(c) The b -value distribution under various search radii (r) from the center of horizontally 0.1° -spacing grids and at least 100 event numbers (n) with the magnitudes greater than an extra cut-off increase of 0.2 in M_c under the given radius. (d) The same as in subfigure (c) but requires the event number of at least 150.

b -value is poorly constrained (Figure 6). Such a b -value uncertainty in the source area offshore can vary similarly to the cases inland under a search radius of 50 km from the epicenter (Figure S3 in Supporting Information S1). Thus, we select the 75% overlapping in this trade-off as reliable results for interpreting the b -value in the source area. Under the 75%-overlapping time windows, the b -value uncertainty can decrease slightly in the source areas inland if the event numbers with their magnitudes over a magnitude threshold increase (Figure S4 in Supporting Information S1). Unfortunately, the temporal resolution of the b -value will be significantly low in the source area. This disadvantage may influence an accurate estimate of the pre-earthquake b -value background level and the possible precursor before the targeted earthquakes. We, therefore, explain the b -value time series surveyed by at least 50 events with their magnitudes over an extra cut-off increase of 0.2 in the precutting level in the source area under a 75% overlapping time window.

We discovered that the b -value in the source area of the 2018 M_L 6.3 Hualien earthquake decreased to 0.69 2 days before it occurred from a pre-earthquake background level of 0.85 ± 0.06 (Figure 7a). The signal is visible

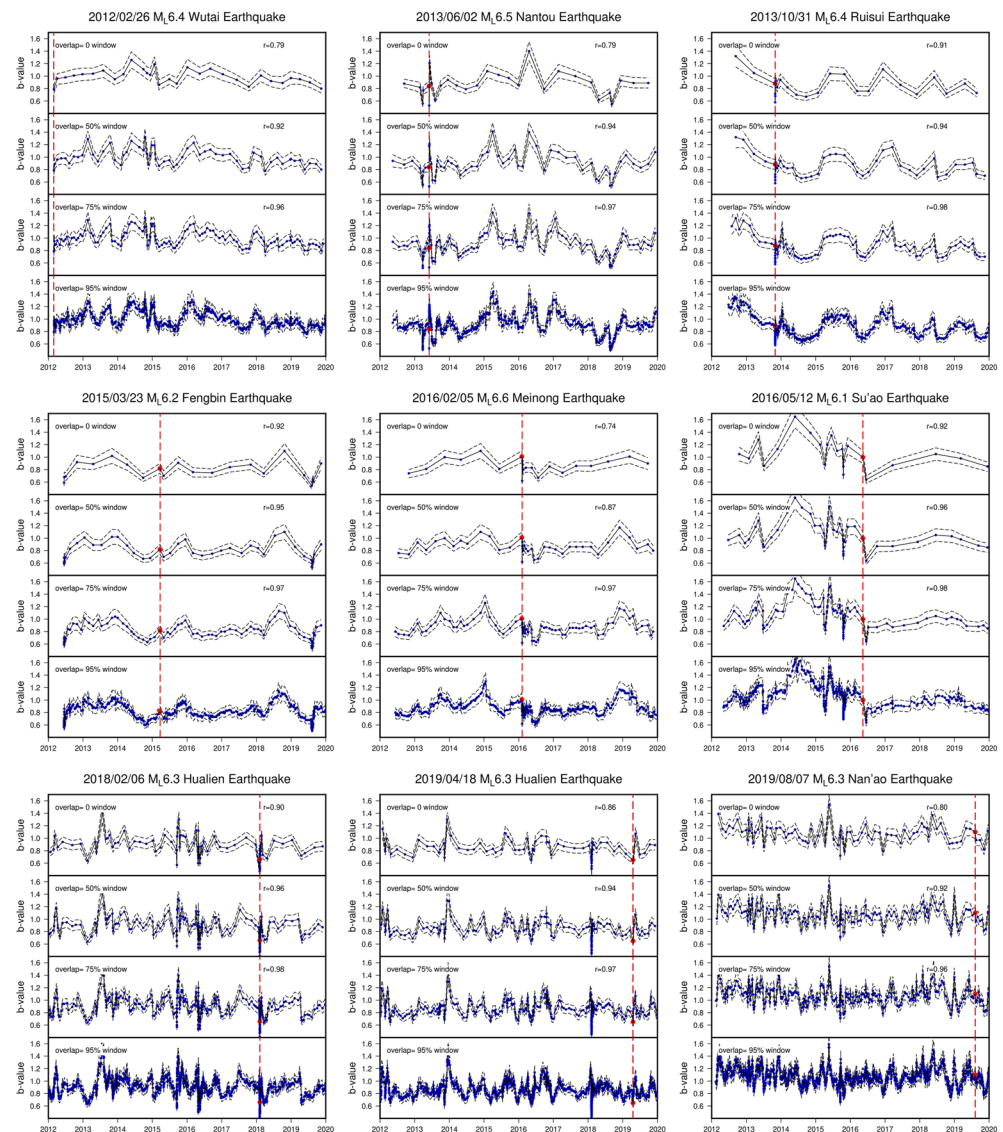


Figure 6. The b -values under a search radius of 20 km from the epicenter of nine targeted $M_L \geq 6.0$ earthquakes with various moving time windows. Each subfigure shows the temporal evolutions of the b -values as blue dots under different overlapping degrees between each time window. The dotted curves represent the uncertainties of the b -values in one standard deviation. The red dotted lines are the earthquake occurrence times. Red circles represent the b -value immediately before the earthquake occurrence.

under another search radius of 50 km from the epicenter, which shows a similar b -value decrease to 0.73 from a pre-earthquake background level of 0.92 ± 0.05 (Figure 7b). Although there is a minor difference between them, such a decrease in both search radiuses is more significant than the uncertainties of the pre-earthquake background level. The signal is still identifiable by a radius of 50 km from the epicenters of the 2015 M_L 6.2 Fengbin and 2019 M_L 6.3 Nan'ao earthquakes in their b -value time series (Figure S5 in Supporting Information S1). The two earthquakes are at least 45 km from the epicenter of the 2018 M_L 6.3 Hualien earthquake (Figure 1) to confirm the robust signal of a b -value decrease. We show the b -value time series surveyed by a radius of 50 km from the epicenter of the other targeted earthquakes in Figure S5 of Supporting Information S1 as evidence and a comparison. In a detail of the b -value precursor, the signal started with a M_L 5.8 earthquake sequence (Figure 7c) that initiated from a location 10 km northeast of the epicenter of the Hualien earthquake. It dropped to 0.57 following a burst of the M_L 5.8 aftershocks and then returned to 0.8 in half a day following the evolution of aftershocks. We found that the b -value decreased again 10 hours before the 2018 M_L 6.3 Hualien earthquake hidden in the b -value time series (Figure 7c). We show stable slopes in the magnitude-frequency relation at the

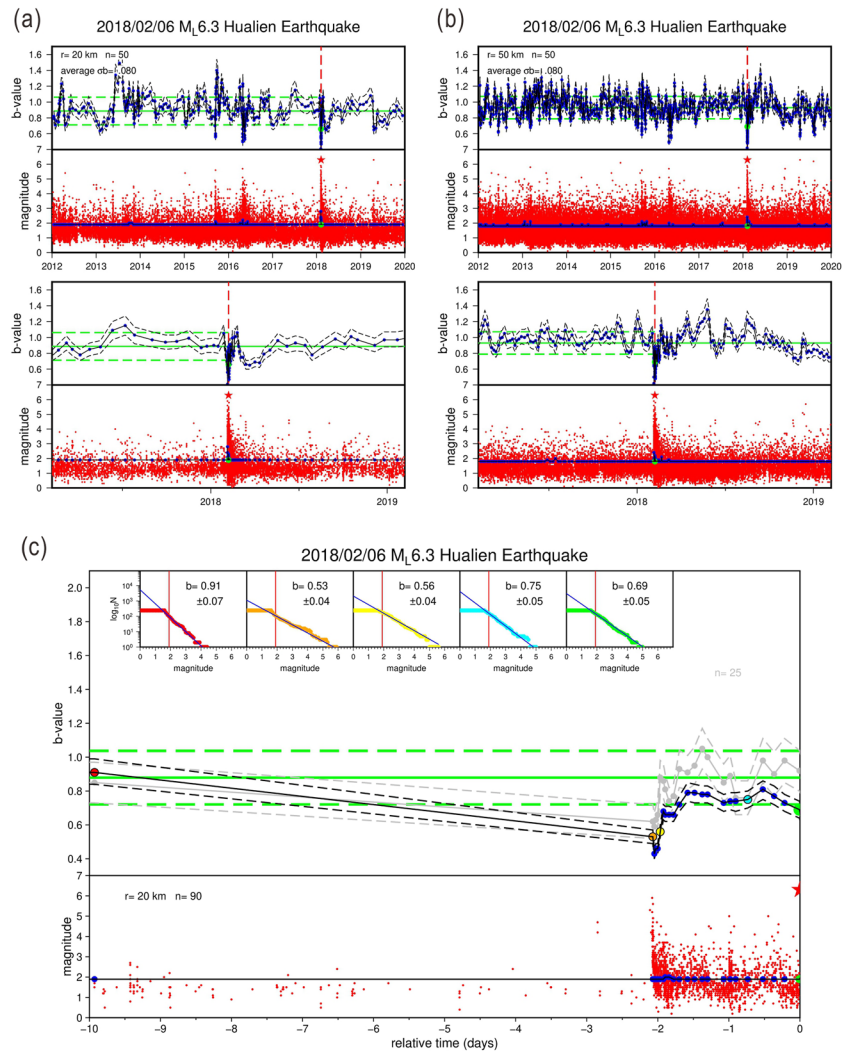


Figure 7. Temporal variations of the b -value and seismicity in the source area of the 2018 M_L 6.3 Hualien earthquake. (a) A search radius of 20 km from the epicenter of the Hualien earthquake for the b -value time series and the seismicity in red small dots. The red star is the earthquake occurrence time. The blue dots represent a temporal evolution of M_C . The green circle represents the b -value immediately before the earthquake occurrence. (b) A radius of 50 km. (c) A viewpoint in 10 days before the Hualien earthquake. The inset subfigures show robust b -value and M_C estimates at the timing of variations. The gray b -value time series denote the solution of B -positive (M_C) in a magnitude difference of 0.2 (van der Elst, 2021).

timing of the b -value variations (Figure 7c) to validate the second decrease, even if it is relatively weak than the first one. The second one in 10 hours coincides with a rapid reduction of $M_L \leq 3.0$ earthquakes in the M_L 5.8 aftershocks (Figure 7c). This phenomenon is consistent with previous findings that the b -value precursor can happen during aftershocks if such a decrease is more significant than the pre-earthquake background level (e.g., Gulia & Wiemer, 2019; Nanjo, 2020; Nanjo et al., 2019). To our knowledge, it is a clear b -value precursor of a large earthquake in space and time from worldwide observations.

We also found a b -value decrease in the source area of the 2013 M_L 6.4 Ruisui and 2016 M_L 6.1 Su'ao earthquakes before their occurrence. In contrast to the 2018 M_L 6.3 Hualien earthquake, the b -value decreased from several months before the two earthquakes without any clear precursor immediately before they occurred (Figure 8). Before the Ruisui earthquake, the b -value decreased to 0.85 at least 8 months ago from the pre-earthquake background level of 1.06 ± 0.08 under a search radius of 20 km. This long-term decrease is visible before the Su'ao earthquake in the b value time series surveyed by the same radius of 20 km. We show the evidence and the time series from the other inland earthquakes as a comparison in Figure 8. The results are consistent with some studies that a large earthquake happens after a long-term decrease in the b -value to imply tectonic stress accumulation on the seismogenic fault (e.g.,

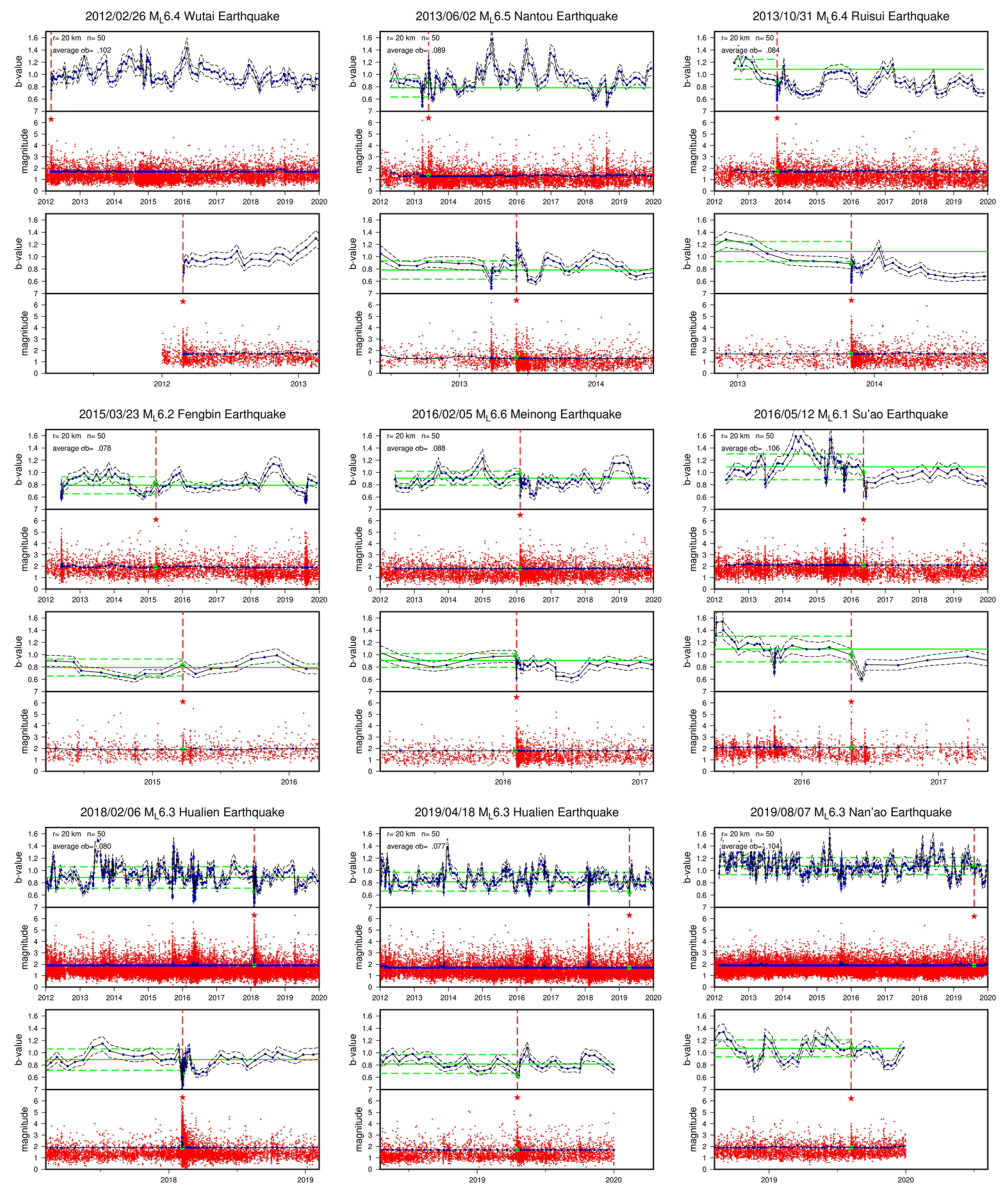


Figure 8. The caption is the same as in Figure 7 but for the other nine targeted inland earthquakes.

Nanjo, 2020; Nanjo et al., 2012; Schurr et al., 2014; Tormann et al., 2015). However, the b -value decrease was less significant before the two Ruisui and Su'ao earthquakes under a search radius of 50 km from the epicenter (Figure S5 in Supporting Information S1). We suggest the signal may be a local phenomenon and needs more observations. Otherwise, we did not find evidence of the b -value precursor in the source area of the other 14 targeted earthquakes in Taiwan. There was some b -value decrease in the 8-year time series but minor and not close to the earthquake occurrence time. They came primarily from the local earthquake sequences or swarms (Figure 8 and Figure S5 in Supporting Information S1). It thus is uncorrelated with either a precursor of the $M_L \geq 6.0$ earthquakes or a potential preslip. Overall, we find no significant variation in the b -value in most cases of Taiwan before large earthquakes.

4. Discussion

4.1. A b -Value Precursor Before the 2018 M_L 6.3 Hualien Earthquake

The b -value precursor was observed to precede a few large earthquakes in the source area and is still an open question in real-time seismology. Before the 2011 M_w 9.0 Tohoku-Oki and 2014 M_w 8.1 Iquique earthquakes,

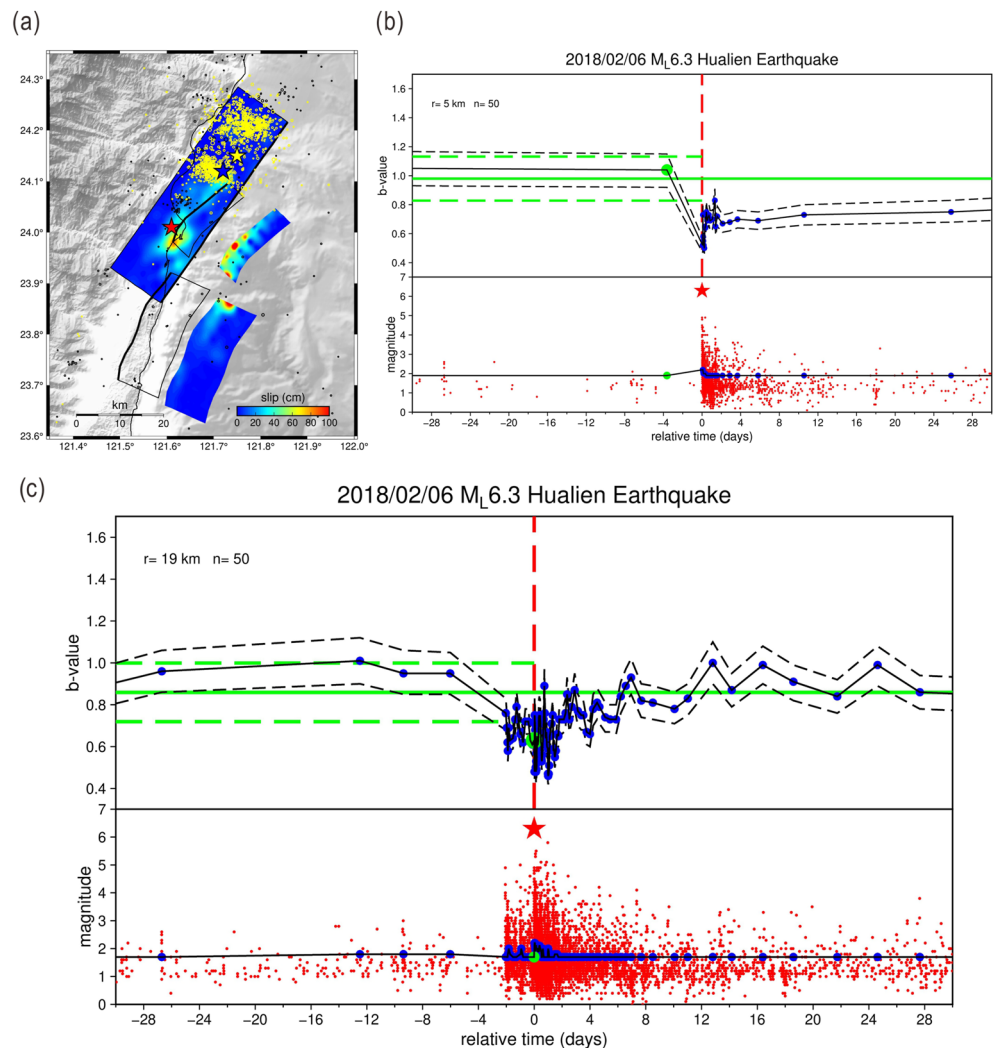


Figure 9. Temporal variations of the b -value and seismicity in a high coseismic slip area from the 2018 M_L 6.3 Hualien earthquake. (a) The coseismic slip distribution on three fault segments (Lee et al., 2018). The red and blue stars represent the epicenters of the M_L 6.3 Hualien earthquake determined by the RMT and CWASN, respectively. The yellow star and circles are an M_L 5.8 earthquake and aftershocks of $M_L \geq 2.0$ within 2 days before the M_L 6.3 Hualien earthquake. The black circles are the background seismicity 1 month before the M_L 6.3 Hualien earthquake. (b) A search radius of 5 km from the RMT epicenter. (c) The search radius lengthens to 19 km.

Schurr et al. (2014) and Tormann et al. (2015) found that the b -value decrease happened primarily in an area of high coseismic slip in the source area, implying the location of earthquake nucleation and initiation (e.g., Toda & Stein, 2022; Wetzler et al., 2018). However, the 2018 M_L 6.3 Hualien earthquake is unique in that the source area did not slip a lot coseismically (the blue star in Figure 9a) but an area 20 km southwestward away on the Milun fault (e.g., Huang & Huang, 2018; Lee et al., 2018). A M_L 5.8 earthquake and its aftershocks within 2 days before the 2018 M_L 6.3 Hualien earthquake are essentially foreshocks (the yellow star and circles in Figure 9a) and in space distinguishable from the high coseismic slip area. Some studies suggested that the high coseismic slip distribution on the Milun fault may be a triggered fault slip by the 2018 M_L 6.3 Hualien earthquake (Lee et al., 2018; Tung et al., 2019). To verify the correlation, we resurveyed the temporal b -value in the high coseismic slip area based on an epicenter released by the Real-Time Moment Tensor Monitoring System (RMT; <https://rmt.earth.sinica.edu.tw/>) (the red star in Figure 9a). In this case, there was no b -value precursor before the 2018 M_L 6.3 Hualien earthquake due to a low seismicity rate at the high coseismic slip area (Figures 9a and 9b). We found the signal only if the search radius is sufficiently long to cover the aftershocks from the M_L 5.8 earthquake in space and time (Figures 9a and 9c). The b -value precursor seems unnecessary to link to a high coseismic

slip area but requires abundant seismicity and clear foreshocks around the epicenter. Van der Elst (2021) proposed a new, more robust method than estimates of the Gutenberg-Richter Law named B-positive, suggesting that the b -value precursors reported by Gulia and Wiemer (2019) and Gulia et al. (2020) before some large earthquakes could be less significant in his B-positive approach. To verify this, we apply the B-positive approach to the source area of the 2018 M_L 6.3 Hualien earthquake and compare the outcome with our results. For the B-positive and B-positive (M_C) estimates, we test the minimum magnitude differences from 0.1 to 0.5 in each time window and constrain the M_C and window length by the same strategy in Section 2. See the definition of B-positive, B-positive (M_C), and determining the magnitude differences in a catalog in van der Elst (2021). The precursor of the b -value decrease we have found does not change significantly under the B-positive strategy (M_C) except for the 0.1 magnitude difference (Figure 7 and Figure S6 in Supporting Information S1). This pattern is consistent with a tiny increase in the temporal M_C value from the precutting level of 1.9–2.0 after the M_L 5.8 earthquake (Figure 7c). Such stability of M_C avoids biasing the b -value by the short-term aftershock incompleteness (van der Elst, 2021) and confirms the precursory signal.

The 2018 M_L 6.3 Hualien earthquake likely ruptured multiple fault segments in the high coseismic slip area and propagated southward during its dynamic process (Lee et al., 2018). This feature, together with the initiation of foreshocks at the downdip of the hypocenter and a southward foreshock migration (Figure 9a), is more of like a cascading rupture process in foreshock-mainshock evolutions (e.g., Ross et al., 2019). However, recent studies found that geodetically detected slow slip and foreshocks preceding large earthquakes can be a preslip process in the source area of large earthquakes (e.g., Ito et al., 2013; Kato et al., 2012; Schurr et al., 2014; Socquet et al., 2017). For example, before the 2011 M_w 9.0 Tohoku-Oki and 2014 M_w 8.1 Iquique earthquakes, there was a remarkable b -value decrease and slow slip in the source area at least 1 month ago and a burst of foreshocks days before the earthquakes. However, no clear b -value precursor was observed immediately before the earthquakes. We showed that the b -value decreased from several months before the 2013 M_L 6.4 Ruisui and 2016 M_L 6.1 Su'ao earthquakes in the source area with no b -value precursor. Although the decrease in the b -value we found was not as significant as observed in those studies, this issue may come from the size of the earthquake itself. The larger the magnitude is, the longer the stress accumulation is required, and so does a remarkable decrease in the b -value. Besides, the foreshocks of the 2018 M_L 6.3 Hualien earthquake seem to initiate at the downdip of the hypocenter, near a source region of $M_w \geq 6.0$ slow slip on the subducting plate interface (Chen et al., 2018, 2022a, 2022b). Slow slip events commonly happen on the fault segment of transitional friction around a high-friction locked zone where large earthquakes reoccur (Bürgmann, 2018; Nishikawa et al., 2019; Obara & Kato, 2016; Saffer & Wallace, 2015). Some foreshocks may have propagated on the preexisting slow slip patch if they were aftershocks of the M_w 5.8 earthquake and followed the afterslip. It may explain the evolution of the foreshocks mostly updip toward the hypocenter of the 2018 M_L 6.3 Hualien earthquake (Figure 9a), nearly identical to the observations from the 2011 M_w 9.0 Tohoku-Oki and 2014 M_w 8.1 Iquique earthquakes. If so, it is crucial to b -value monitoring in the source area of the 2018 M_L 6.3 Hualien earthquake and the downdip slow slip patch if the precursor returns. Note the afterslip of the M_w 5.8 earthquake is out of the scope of this study, could be tiny on the geodetic time series, and needs more analysis in the future.

4.2. Temporal Variations of the b -Value After $M_L \geq 6.0$ Earthquakes

Gulia et al. (2018) found that the b -value can increase immediately after worldwide M_w 6.0 to 8.0 earthquakes in the fault zone and decrease in the evolution of linear to exponential decay, returning to the pre-earthquake background level. However, our observations for the b -value in Taiwan are unlike the findings of Gulia et al. (2018) in most cases after the $M_L \geq 6.0$ earthquakes. There is only one case in which the b -value increased immediately in the source area of the 2013 M_L 6.5 Nantou earthquake after it occurred (Figure S5 in Supporting Information S1). We found that the temporal b -value vibrated irregularly in an uncertainty of the pre-earthquake background level in the source area of most targeted earthquakes after they occurred. The temporal b -value, sometimes, can decrease immediately after the earthquakes and return to the pre-earthquake background level during the aftershocks (Figure S5 in Supporting Information S1). In these cases, we found that the b -value decrease correlates with a burst of the $M_L \geq 2.0$ aftershocks at the beginning of the aftershock sequence. Such a return in the b -value seems to be related to a reduction of the $M_L \geq 2.0$ aftershocks (Figure S5 in Supporting Information S1). In Figure 10, we show a case of the b -value decreasing immediately after the 2018 M_L 6.3 Hualien earthquake and recovering with time in the source area with robust estimates of the b -values at the timing of variations. The aftershock sequence typically follows a decay rate of the Omori-Law in the number

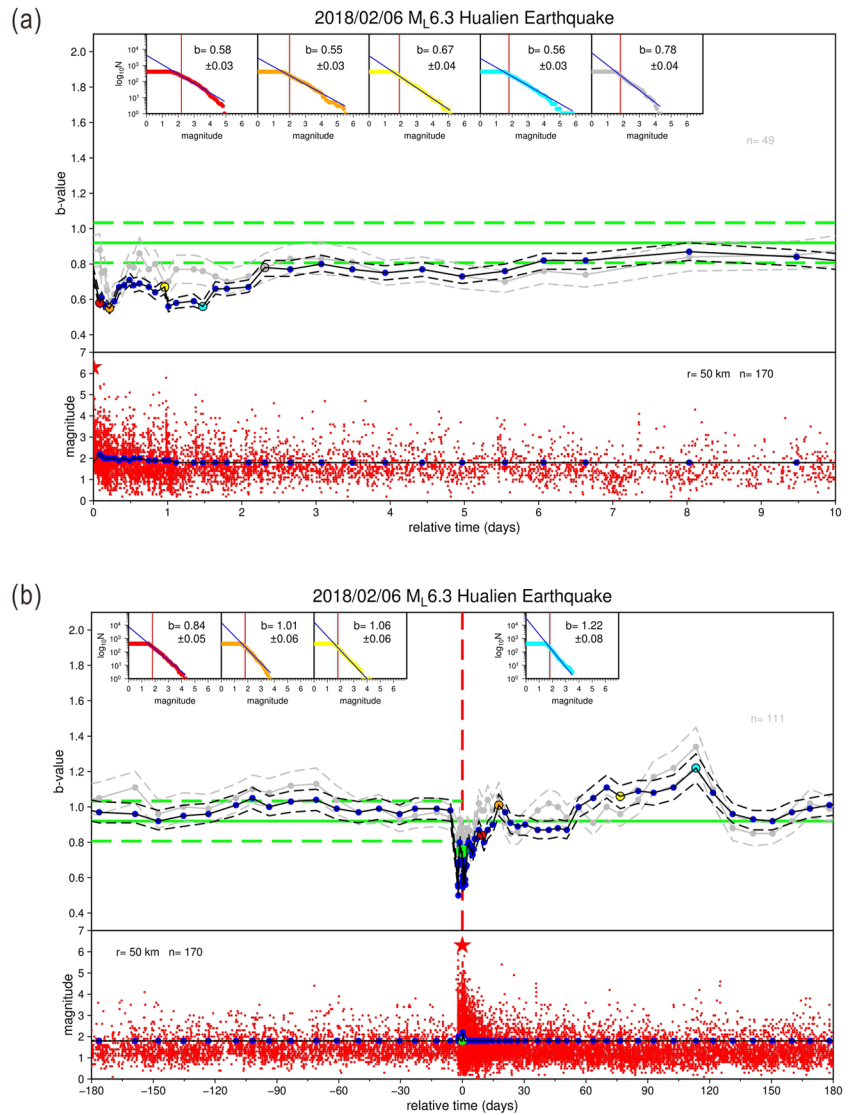


Figure 10. Temporal evolution of the b -value targeting the aftershocks of the 2018 M_L 6.3 Hualien earthquake. (a) A viewpoint in 10 days after the M_L 6.3 Hualien earthquake and for 3 months later in (b). The gray b -value time series denote the solution of B -positive in a magnitude difference of 0.2 (van der Elst, 2021). The other captions are the same as in Figure 7.

and magnitude of $M_L \geq 2.0$ events, almost as the threshold of temporal M_C in the catalog (Figure 10). We think it is representative of the temporal b -value evolution during aftershocks. Note that the B -positive method can reproduce a decrease of the b -value immediately after the 2018 M_L 6.3 Hualien earthquake and recover to the pre-earthquake background level (Figure 10 and Figure S6 in Supporting Information S1). Our observations of no increase in the b -value after a large earthquake are consistent with recent studies in Southern California, Japan, and Italy (García-Hernández et al., 2021; Gulia & Wiemer, 2019; Nanjo et al., 2019; van der Elst, 2021). The difference in the evolution of the b -value is probably critical in a strategy of spatial search criteria on aftershocks. Gulia et al. (2018) defined aftershocks as the seismicity in and around the fault zone where a large earthquake has ruptured coseismically. However, the behaviors of aftershocks can vary with faulting styles and not only narrow down in the preexisting fault zone after great earthquakes (e.g., Toda & Stein, 2022; Wetzler et al., 2018). A bias of the b -value can happen in the early aftershocks due to a significant increase in the M_C in the catalog as a short-term aftershock incompleteness (van der Elst, 2021). We have verified that a search radius of 50 km from the epicenter is capable of a b -value mapping during aftershocks of a large earthquake in Taiwan. Our b -value survey is stably under a low M_C of less than 2.0 in the source area of most $M_L \geq 6.0$ earthquakes, and the M_C did

not increase significantly during the aftershocks in most cases (Figures 9 and 10 and Figure S5 in Supporting Information S1). It better explains the magnitude-frequency relation of small to large earthquakes during aftershocks, compared to Gulia et al. (2018), primarily under a b -value survey from a higher M_C of 3.0–4.0. We note, however, that all the targeted earthquakes we analyzed in Taiwan are less than a magnitude of M_L 6.7. Studying larger-magnitude earthquakes is needed for stress changes in the early aftershocks, linked to the critical issue of triggering an impending surrounding great event.

In this study, we did not find clear evidence of a b -value decrease during the aftershocks of all targeted earthquakes in Taiwan. This observation agrees with truth in all cases: no large earthquakes occur in the surrounding fault asperities during the aftershocks if no b -value decrease can be observed (e.g., Gulia & Wiemer, 2019; Nanjo, 2020; Nanjo et al., 2019). We only found that the b -value decreased before the 2018 M_L 6.3 Hualien earthquake and after a M_L 5.8 earthquake within 2 days during the aftershocks (Figures 7, 9a, and 9c). However, neither our moving time-windows strategy nor the B-positive method (van der Elst, 2021) can distinguish spontaneous or triggered aftershocks from seismicity. Spontaneous aftershocks may correlate with a region of the Coulomb stress increase after a large earthquake. Triggered aftershocks may primarily come from the dynamic seismic waves (e.g., Hardebeck, 2022; Toda & Stein, 2022). An evolution of spontaneous aftershocks in space and time should be more closely related to assessing impending large earthquakes. Our little understanding of the two-type aftershocks makes it hard to identify whether the events are spontaneous. It may be a reason for temporal irregular b -values that happened after most targeted earthquakes in our systematic survey. Hence, the evolution of aftershock b -values needs a more accurate estimate focused on spontaneous-type events with no short-term aftershock incompleteness.

4.3. Effectivity of Moving Time-Windows Survey and Perspective

In this study, we showed the moving time-windows survey is a simple and efficient way to monitor the b -value precursor of a large earthquake in Taiwan. Our results agree with previous worldwide findings that the spatiotemporal search criteria for the b -value are critical in what you will see in the b -value time series (Chen & Zhu, 2020; García-Hernández et al., 2021; Gulia et al., 2018; Tormann et al., 2015; van der Elst, 2021). A high-resolution b -value time series that satisfies a linkage to large earthquakes without misinterpretation requires careful studies of the magnitude-frequency relation. Our observations support the detectability of b -value precursor by present instrumental capacities, even if it could be the end phase of a preslip process. Preslip before large earthquakes in the source area can begin earlier than the foreshocks/ b -value precursor from several weeks to months. This phenomenon has been well-documented in the cases of the 2011 M_w 9.0 Tohoku-Oki and 2014 M_w 8.1 Iquique earthquakes, depicted primarily by geodetic and seismologic joint observations (Ito et al., 2013; Kato et al., 2012; Ruiz et al., 2014; Schurr et al., 2014; Socquet et al., 2017). The preslip initiated aseismically in the downdip area of the earthquake hypocenter, migrated upward with time, and likely accelerated with intense foreshocks in the end phase. Some preslip can even be aseismic till the earthquake occurrence with no foreshocks, as observed in the 2014 M_w 7.3 Papanoa and 2018 M_w 6.9 Zakynthos earthquakes (Radigue et al., 2016; Saltogianni et al., 2021). We suggest that b -value precursor studies need auxiliary geodetic observations to fill a possible aseismic gap in an entire seismogenic fault to find the nucleation zone earlier. The preslip and its related stress dynamics could be identified more effectively by improvements in the measurements' precision and density.

5. Conclusions

This study performs a high-quality temporal b -value survey in Taiwan in the source area of $M_L \geq 6.0$ earthquakes. We found that the b -value decreased for 2 days before the 2018 M_L 6.3 Hualien earthquake as a robust precursor. This signal is more significant than the pre-earthquake background b -value level and independent of the choice of search criteria on seismicity in space and time. Such a decrease in the b -value coincided with the timing of foreshocks (a M_L 5.8 earthquake and its aftershocks) nearby and at a downdip of the hypocenter of the 2018 M_L 6.3 Hualien earthquake. We found the b -value returned to the pre-earthquake background level following an evolution of the foreshocks toward updip the hypocenter of the 2018 M_L 6.3 Hualien earthquake. We found a second decrease in the b -value 10 hours before the earthquake occurred that coincided with a rapid reduction of small earthquakes at the nucleation zone. This observation seems to agree with recent findings of preslip immediately before a large earthquake. The b -value can decrease from several months before the 2013 M_L 6.4 Ruisui and 2016 M_L 6.1 Su'ao earthquakes in the source area. However, the signal seems localized in space

and has no b -value precursor in the two cases. Otherwise, there is no evidence of a b -value precursor before the targeted earthquakes in the source area and during the aftershocks. The observations are consistent with the truth in the 17 earthquakes: Only the 2018 M_L 6.3 Hualien earthquake has a foreshock sequence. No impending large earthquakes occurred nearby any of the 17 earthquakes during aftershocks. This study provides direct evidence for the b -value precursor in space and time and promotes real-time monitoring progressively.

Data Availability Statement

The catalog of the relocated earthquakes used for the b -value analysis is available at <http://seismology.gi.ntu.edu.tw/download.htm>.

Acknowledgments

We appreciate the Editor and two anonymous reviewers for constructive comments to improve the manuscript. We thank the Central Weather Administration for providing the earthquake data that can be used for relocation work and b -value analysis. This study was funded by the Ministry of Science and Technology (MOST) in Taiwan under Grant 112-2116-M-002-024.

References

- Aki, K. (1965). Maximum likelihood estimate of b in the formula $\log N = a - bM$ and its confidence. *Bulletin of the Seismological Society of America*, 43, 237–239.
- Amitrano, D. (2003). Brittle-ductile transition and associated seismicity: Experimental and numerical studies and relationship with the b value. *Journal of Geophysical Research*, 108(B1), 2044. <https://doi.org/10.1029/2001JB000680>
- Bilek, S. L., & Lay, T. (2018). Subduction zone megathrust earthquakes. *Geosphere*, 14(4), 1468–1500. <https://doi.org/10.1130/GES01608.1>
- Bürgmann, R. (2018). The geophysics, geology and mechanics of slow fault slip. *Earth and Planetary Science Letters*, 495, 112–134. <https://doi.org/10.1016/j.epsl.2018.04.062>
- Chan, C. H., Wu, Y. M., Tseng, T. L., Lin, T. L., & Chen, C. C. (2012). Spatial and temporal evolution of b -values before large earthquakes in Taiwan. *Tectonophysics*, 532–535, 215–222. <https://doi.org/10.1016/j.tecto.2012.02.004>
- Chen, J., & Zhu, S. (2020). Spatial and temporal b -value precursors preceding the 2008 Wenchuan, China, earthquake ($M_w = 7.9$): Implications for earthquake prediction. *Geomatics, Natural Hazards and Risk*, 11(1), 1196–1211. <https://doi.org/10.1080/19475705.2020.1784297>
- Chen, S. K., Wu, Y. M., & Chan, Y. C. (2018). Episodic slow slip events and overlying plate seismicity at the southernmost Ryukyu Trench. *Geophysical Research Letters*, 45(19), 10369–10377. <https://doi.org/10.1029/2018GL079740>
- Chen, S. K., Wu, Y. M., & Chan, Y. C. (2022a). Slow slip events following the afterslip of the 2002 M_w 7.1 Hualien offshore earthquake, Taiwan. *Earth Planets and Space*, 74(1), 63. <https://doi.org/10.1186/s40623-022-01629-y>
- Chen, S. K., Wu, Y. M., & Chan, Y. C. (2022b). The seismogenic potential of the southernmost Ryukyu subduction zone as revealed by historical earthquakes and slow slip events. *Frontiers in Earth Science*, 10, 887182. <https://doi.org/10.3389/feart.2022.887182>
- Chen, S. K., Wu, Y. M., Hsu, Y. J., & Chan, Y. C. (2017). Current crustal deformation reassessed by cGPS strain-rate estimation and focal mechanism stress inversion. *Geophysical Journal International*, 210(1), 228–239. <https://doi.org/10.1093/gji/ggx165>
- Dal Zillo, L., van Dinther, Y., Gerya, T. V., & Pranger, C. C. (2018). Seismic behaviour of mountain belts controlled by plate convergence rate. *Earth and Planetary Science Letters*, 482, 81–92. <https://doi.org/10.1016/j.epsl.2017.10.053>
- García-Hernández, R., D'Auria, L., Barrancos, J., Padilla, G. D., & Pérez, N. M. (2021). Multiscale temporal and spatial estimation of the b -Value. *Seismological Research Letters*, 92(6), 3712–3724. <https://doi.org/10.1785/0220200388>
- Goebel, T. H. W., Schorlemmer, D., Becker, T. W., Dresen, G., & Sammis, C. G. (2013). Acoustic emissions document stress changes over many seismic cycles in stick-slip experiments. *Geophysical Research Letters*, 40(10), 2049–2054. <https://doi.org/10.1002/grl.50507>
- Gulia, L., Rinaldi, A. P., Tormann, T., Vannucci, G., Enescu, B., & Wiemer, S. (2012). The effect of a mainshock on the size distribution of the aftershocks. *Geophysical Research Letters*, 45(24), 13277–13287. <https://doi.org/10.1029/2018GL080619>
- Gulia, L., & Wiemer, S. (2019). Real-time discrimination of earthquake foreshocks and aftershocks. *Nature*, 574(7777), 193–199. <https://doi.org/10.1038/s41586-019-1606-4>
- Gulia, L., Wiemer, S., & Vannucci, G. (2020). Pseudoprospective evaluation of the foreshock traffic-light system in Ridgecrest and implications for aftershock hazard assessment. *Seismological Research Letters*, 91(5), 2828–2842. <https://doi.org/10.1785/0220190307>
- Gutenberg, B., & Richter, C. F. (1944). Frequency of earthquake in California. *Bullet of the Seismological Society of America*, 34(4), 185–188. <https://doi.org/10.1785/bssa0340040185>
- Hardebeck, J. L. (2022). Physical properties of the crust influence aftershock locations. *Journal of Geophysical Research*, 127(10), e2022JB024727. <https://doi.org/10.1029/2022JB024727>
- Hashimoto, C., Noda, A., Sagiya, T., & Matsu'ura, M. (2009). Interplate seismogenic zones along the Kuril–Japan trench inferred from GPS data inversion. *Nature Geoscience*, 2(2), 141–144. <https://doi.org/10.1038/ngeo421>
- Hsu, Y. J., Yu, S. B., Simons, M., Kuo, L. C., & Chen, H. Y. (2009). Interseismic crustal deformation in the Taiwan plate boundary zone revealed by GPS observations, seismicity, and earthquake focal mechanisms. *Tectonophysics*, 479(1–2), 4–18. <https://doi.org/10.1016/j.tecto.2008.11.016>
- Huang, H. H., Wu, Y. M., Song, X. D., Chang, C. H., Lee, S. C., Chang, T. M., & Hsieh, H. H. (2014). Joint V_p and V_s tomography of Taiwan: Implications for subduction-collision orogeny. *Earth and Planetary Science Letters*, 392, 177–191. <https://doi.org/10.1016/j.epsl.2014.02.026>
- Huang, M. H., & Huang, H. H. (2018). The complexity of the 2018 M_w 6.4 Hualien earthquake in east Taiwan. *Geophysical Research Letters*, 45(13), 257. 249–13. <https://doi.org/10.1029/2018GL080821>
- Ito, Y., Hino, R., Kido, M., Fujimoto, H., Osada, Y., Inazu, D., et al. (2013). Episodic slow slip events in the Japan subduction zone before the 2011 Tohoku-Oki earthquake. *Tectonophysics*, 600, 14–26. <https://doi.org/10.1016/j.tecto.2012.08.022>
- Kato, A., Obara, K., Igarashi, T., Tsuruoka, H., Nakagawa, S., & Hirata, N. (2012). Propagation of slow slip leading up to the 2011 M_w 9.0 Tohoku-Oki earthquake. *Science*, 335, 705–708. <https://doi.org/10.1126/science.1215141>
- Kuo-Chen, H., Wu, F. T., & Roecker, S. W. (2012). Three-dimensional P velocity structures of the lithosphere beneath Taiwan from the analysis of TAIGER and related seismic data sets. *Journal of Geophysical Research*, 117(B6), B06306. <https://doi.org/10.1029/2011JB009108>
- Lee, S. J., Lin, T. C., Liu, T. Y., & Wong, T. P. (2018). Fault-to-fault jumping rupture of the 2018 M_w 6.4 Hualien Earthquake in eastern Taiwan. *Seismological Research Letters*, 90(1), 30–39. <https://doi.org/10.1785/0220180182>
- Lee, Y. T., Turcotte, D. L., Rundle, J. B., & Chen, C. C. (2013). Aftershock statistics of the 1999 Chi–Chi, Taiwan earthquake and the concept of Omori times. *Pure and Applied Geophysics*, 170(1), 221–228. <https://doi.org/10.1007/s00024-011-0445-5>
- Nanjio, K. Z. (2020). Were changes in stress state responsible for the 2019 Ridgecrest, California, earthquakes? *Nature Communications*, 11(1), 3082. <https://doi.org/10.1038/s41467-020-16867-5>

- Nanjo, K. Z., Hirata, N., Obara, K., & Kasahara, K. (2012). Decade-scale decreases in b value prior to the M9-class 2011 Tohoku and Sumatra quakes. *Geophysical Research Letters*, 39(20), L20304. <https://doi.org/10.1029/2012GL052997>
- Nanjo, K. Z., Izutsu, J., Orihara, Y., Kamogawa, M., & Nagao, T. (2019). Changes in seismicity pattern due to the 2016 Kumamoto earthquakes identify a highly stressed area on the Hinagu fault zone. *Geophysical Research Letters*, 46(16), 9489–9496. <https://doi.org/10.1029/2019GL083463>
- Nanjo, K. Z., & Yoshida, A. (2018). A b map implying the first eastern rupture of the Nankai Trough earthquakes. *Nature Communications*, 9(1), 1117. <https://doi.org/10.1038/s41467-018-03514-3>
- Nishikawa, T., Matsuzawa, T., Ohta, K., Uchida, N., Nishimura, T., & Ide, S. (2019). The slow earthquake spectrum in the Japan Trench illuminated by the S-net seafloor observatories. *Science*, 365(6455), 808–813. <https://doi.org/10.1126/science.aax5618>
- Obara, K., & Kato, A. (2016). Connecting slow earthquakes to huge earthquakes. *Science*, 353(6296), 253–257. <https://doi.org/10.1126/science.aaf1512>
- Petrucelli, A., Schorlemmer, D., Tormann, T., Rinaldi, A. P., Wiemer, S., Gasperini, P., & Vannucci, G. (2019). The influence of faulting style on the size-distribution of global earthquakes. *Earth and Planetary Science Letters*, 527, 115719. <https://doi.org/10.1016/j.epsl.2019.115791>
- Radiguet, M., Perfettini, H., Cotte, N., Gualandi, A., Valette, B., Kostoglodov, V., et al. (2016). Triggering of the 2014 M_w 7.3 Papanoa earthquake by a slow slip event in Guerrero, Mexico. *Nature Geoscience*, 9(11), 829–833. <https://doi.org/10.1038/ngeo2817>
- Ross, Z. E., Idini, B., Jia, Z., Stephenson, O. L., Zhong, M., Wang, X., et al. (2019). Hierarchical interlocked orthogonal faulting in the 2019 Ridgecrest earthquake sequence. *Science*, 366(6463), 346–351. <https://doi.org/10.1126/science.aaz0109>
- Ruiz, S., Metois, M., Fuenzalida, A., Ruiz, J., Leyton, F., Grandin, R., et al. (2014). Intense foreshocks and a slow slip event preceded the 2014 Iquique M_w 8.1 earthquake. *Science*, 345(6201), 1165–1169. <https://doi.org/10.1126/science.1256074>
- Saffer, D. M., & Wallace, L. M. (2015). The frictional, hydrologic, metamorphic and thermal habitat of shallow slow earthquakes. *Nature Geoscience*, 8, 594–600. <https://doi.org/10.1038/ngeo2490>
- Saltogian, V., Mouslopoulou, V., Dielforder, A., Bocchini, G. M., Bedford, J., & Oncken, O. (2021). Slow slip triggers the 2018 M_w 6.9 Zakynthos earthquake within the weakly locked Hellenic subduction system, Greece. *Geochemistry, Geophysics, Geosystems*, 22(11), e2021GC010090. <https://doi.org/10.1029/2021GC010090>
- Scholz, C. H. (1968). The frequency-magnitude relation of microfracturing in rock and its relation to earthquakes. *Bullet of the Seismological Society of America*, 58(1), 399–415. <https://doi.org/10.1785/bssa0580010399>
- Scholz, C. H. (2015). On the stress dependence of the earthquake b value. *Geophysical Research Letters*, 42(5), 1399–1402. <https://doi.org/10.1002/2014GL062863>
- Schorlemmer, D., Wiemer, S., & Wyss, M. (2005). Variations in earthquake-size distribution across different stress regimes. *Nature*, 437(7058), 539–542. <https://doi.org/10.1038/nature04094>
- Schurr, B., Asch, G., Hainzl, S., Bedford, J., Hoechner, A., Palo, M., et al. (2014). Gradual unlocking of plate boundary controlled initiation of the 2014 Iquique earthquake. *Nature*, 512(7514), 299–302. <https://doi.org/10.1038/nature13681>
- Shi, Y., & Bolt, B. A. (1982). The standard error of the magnitude-frequency b value. *Bulletin of the Seismological Society of America*, 72(5), 1677–1687. <https://doi.org/10.1785/BSSA0720051677>
- Socquet, A., Valdes, J. P., Jara, J., Cotton, F., Walpersdorf, A., Cotte, N., et al. (2017). An 8 month slow slip event triggers progressive nucleation of the 2014 Chile megathrust. *Geophysical Research Letters*, 44(9), 4046–4053. <https://doi.org/10.1002/2017GL073023>
- Spada, M., Tormann, T., Wiemer, S., & Enescu, B. (2013). Generic dependence of the frequency-size distribution of earthquakes on depth and its relation to the strength profile of the crust. *Geophysical Research Letters*, 40(4), 709–714. <https://doi.org/10.1029/2012GL054198>
- Toda, S., & Stein, R. S. (2022). Central shutdown and surrounding activation of aftershocks from megathrust earthquake stress transfer. *Nature Geoscience*, 15(6), 494–500. <https://doi.org/10.1038/s41561-022-00954-x>
- Tormann, T., Enescu, B., Woessner, J., & Wiemer, S. (2015). Randomness of megathrust earthquakes implied by rapid stress recovery after the Japan earthquake. *Nature Geoscience*, 8(2), 152–158. <https://doi.org/10.1038/ngeo2343>
- Tung, H., Chen, H. Y., Hsu, Y. J., Hu, J. C., Chang, Y. H., & Kuo, Y. T. (2019). Triggered slip on multifaults after the 2018 M_w 6.4 Hualien earthquake by continuous GPS and InSAR measurements. *Terrestrial, Atmospheric and Oceanic Sciences*, 30(3), 285–300. <https://doi.org/10.3319/TAO.2019.04.03.01>
- van der Elst, N. J. (2021). B-Positive: A robust estimator of aftershock magnitude distribution in transiently incomplete catalogs. *Journal of Geophysical Research: Solid Earth*, 126(2). <https://doi.org/10.1029/2020jb021027>
- Wang, J. H. (1988). b values of shallow earthquakes in Taiwan. *Bulletin of the Seismological Society of America*, 78(3), 1243–1254. <https://doi.org/10.1785/BSSA0780031243>
- Wang, J. H., Chen, K. C., Leu, P. L., & Chang, J. H. (2015). b -values observations in Taiwan: A review. *Terrestrial, Atmospheric and Oceanic Sciences*, 26(5), 475. [https://doi.org/10.3319/TAO.2015.04.28.01\(T\)](https://doi.org/10.3319/TAO.2015.04.28.01(T))
- Wetzler, N., Lay, T., Brodsky, E. E., & Kanamori, H. (2018). Systematic deficiency of aftershocks in areas of high coseismic slip for large subduction zone earthquakes. *Science Advances*, 4(2), eaao3225. <https://doi.org/10.1126/sciadv.aao3225>
- Wiemer, S., & Wyss, M. (1997). Mapping the frequency-magnitude distribution in asperities: An improved technique to calculate recurrence times? *Journal of Geophysical Research*, 102(B7), 15115–15128. <https://doi.org/10.1029/97JB00726>
- Wiemer, S., & Wyss, M. (2000). Minimum magnitude of completeness in earthquake catalogs: Examples from Alaska, the Western United States, and Japan. *Bullet of the Seismological Society of America*, 90(4), 859–869. <https://doi.org/10.1785/0119990114>
- Woessner, J., & Wiemer, S. (2005). Assessing the quality of earthquake catalogues: Estimating the magnitude of completeness and its uncertainty. *Bullet of the Seismological Society of America*, 95(2), 684–698. <https://doi.org/10.1785/0120040007>
- Wu, Y. H., Chen, C. C., Turcotte, D. L., & Rundle, J. B. (2013). Quantifying the seismicity on Taiwan. *Geophysical Journal International*, 194(1), 465–469. <https://doi.org/10.1093/gji/ggt101>
- Wu, Y. M., Chang, C. H., Zhao, L., Shyu, J. B. H., Chen, Y. G., Sieh, K., & Avouac, J. P. (2007). Seismic tomography of Taiwan: Improved constraints from a dense network of strong motion stations. *Journal of Geophysical Research*, 112(B8). <https://doi.org/10.1029/2007JB004983>
- Wu, Y. M., Chang, C. H., Zhao, L., Teng, T. L., & Nakamura, M. (2008b). A comprehensive relocation of earthquakes in Taiwan from 1991 to 2005. *Bulletin of the Seismological Society of America*, 98(3), 1471–1481. <https://doi.org/10.1785/0120070166>
- Wu, Y. M., Chen, C. C., Zhao, L., & Chang, C. H. (2008). Seismicity characteristics before the 2003 Chengkung, Taiwan, earthquake. *Tectonophysics*, 457(3–4), 177–182. <https://doi.org/10.1016/j.tecto.2008.06.007>
- Wu, Y. M., Chen, S. K., Huang, T. C., Huang, H. H., Chao, W. A., & Koulakov, I. (2018). Relationship between earthquake b -values and crustal stresses in a young orogenic belt. *Geophysical Research Letters*, 45(4), 1832–1837. <https://doi.org/10.1002/2017GL076694>
- Wu, Y. M., & Chiao, L. Y. (2006). Seismic quiescence before the 1999 Chi-Chi, Taiwan M_w 7.6 earthquake. *Bulletin of the Seismological Society of America*, 96(1), 321–327. <https://doi.org/10.1785/0120050069>
- Yu, S. B., Chen, H. Y., & Kuo, L. C. (1997). Velocity field of GPS stations in the Taiwan area. *Tectonophysics*, 274(1–3), 41–59. [https://doi.org/10.1016/S0040-1951\(96\)00297-1](https://doi.org/10.1016/S0040-1951(96)00297-1)